# Supplemental Figure 1

**A**

**CITE-seq sample dataset**

| | |
|---|---|
| Recent-Onset (RO) | n = 4 |
| anti-CD3 Responders (R) | n = 4 |
| anti-CD3 Non-Responders (NR) | n = 3 |
| total | n = 11 |

**B**

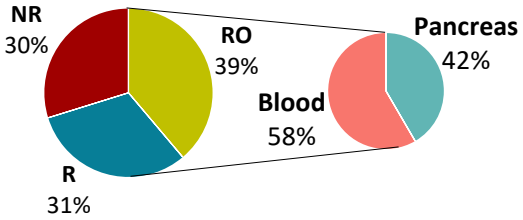


**Supplemental Figure 1. CITE-sequencing dataset composition.** (**A**) Biological condition and number of samples used for CITE-sequencing. (**B**) Diagram showing the proportion of cells derived from both blood and pancreas across RO (Recent-Onset), R (Responder), and NR (Non-Responder) mice. All proportions are normalized to the total cell count in the dataset.

# Supplemental Figure 2

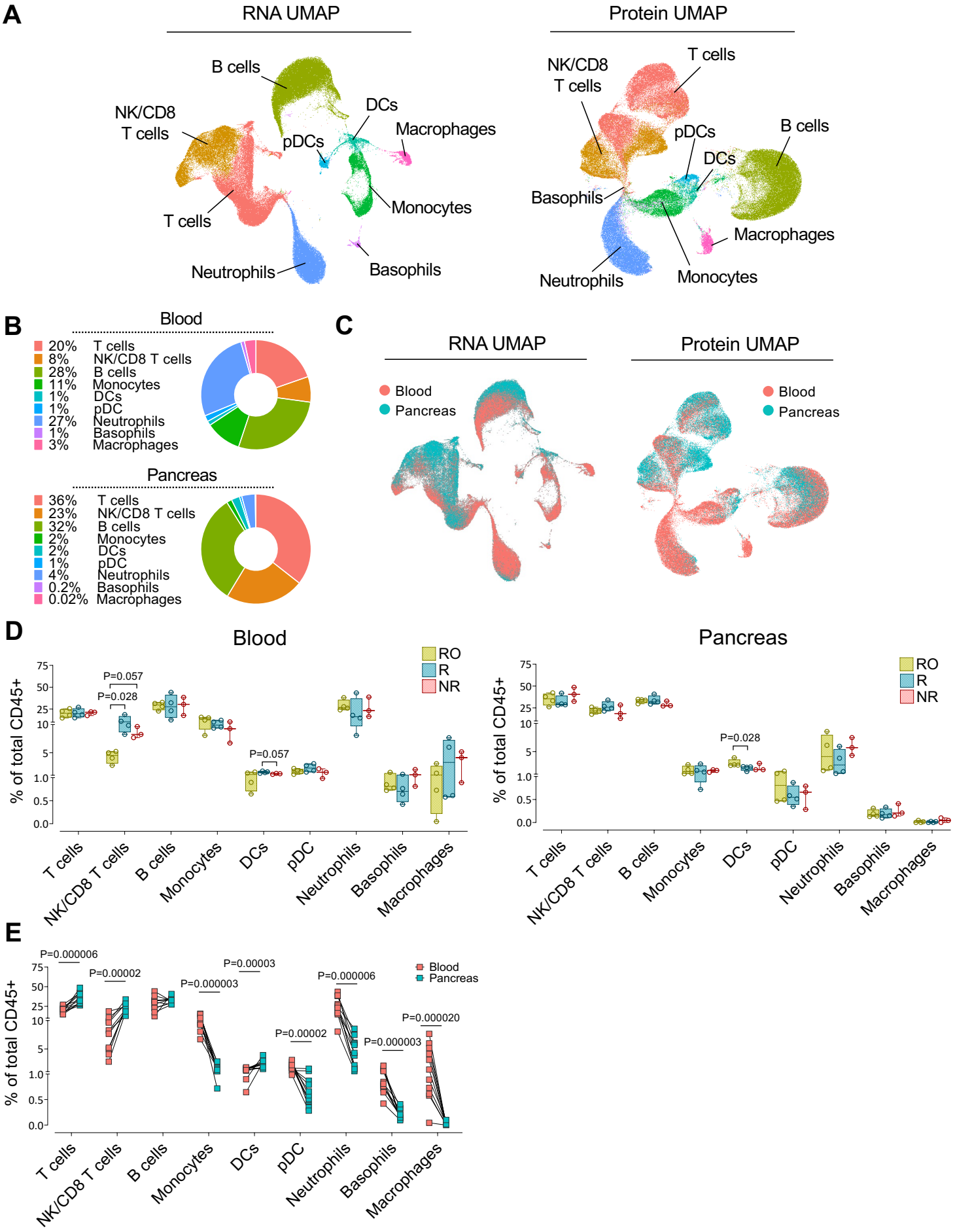

**Supplemental Figure 2. Immune subset profiling in peripheral blood and pancreas of NOD mice.** (**A**) UMAP (Uniform Manifold Approximation and Projection) visualizations of immune cell populations computed using RNA (left) or proteins (right). Cell types were identified using top variable genes and proteins. (**B**) Diagrams showing the proportions of the immune cell populations in peripheral blood and pancreas. (**C**) UMAP plot of immune cells colored according to their tissue of origin, with peripheral blood cells represented in red and pancreas cells in green. (**D**) Box plots showing the frequency of major immune cell types in RO (Recent-Onset; yellow), R (Responder; blue), NR (Non-Responder; red) samples, normalized on total counts of $CD45^+$ leukocytes. Boxes represent the median (center line) and extend from the $25^{th}$ to $75^{th}$ percentiles (bottom and top lines, respectively); whiskers extend from the minimum to the maximum value. (**E**) Slope chart showing the frequencies of each cell type in paired peripheral blood (red) and pancreas (green) samples for each mouse of the CITE-seq dataset. In (**D, E**), the Mann-Whitney U test was used for statistical comparison.

# Supplemental Figure 3

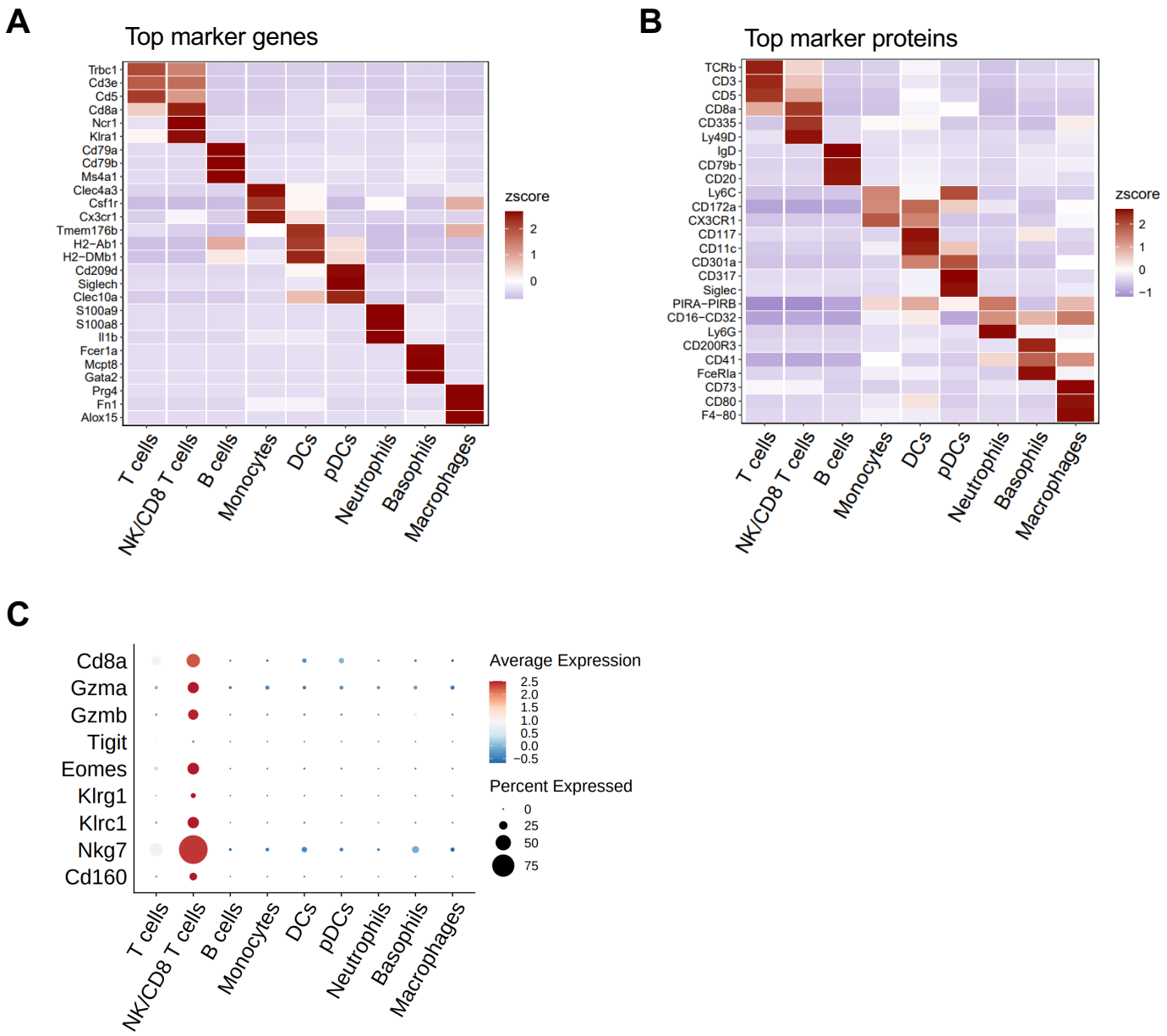


**Supplemental Figure 3. Unsupervised immune subset clustering based on RNA and protein markers in mouse peripheral blood and pancreas samples.** Heat map showing the expression of top marker genes (**A**) or proteins (**B**) in the main immune cell types in both peripheral blood and pancreas. (**C**) Dot plot illustrating the expression of genes associated with partial exhaustion phenotype.

## Supplemental Figure 4

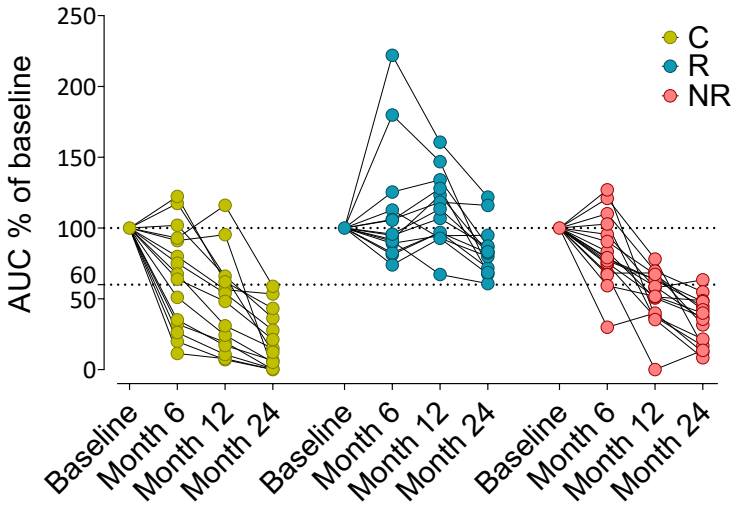


**Supplemental Figure 4. C-peptide AUC percentage after teplizumab therapy in new-onset type 1 diabetes.** Dot plot illustrating the percentage of C-peptide levels, measured as the mean AUC (Area Under the Curve), at baseline, and 6, 12, and 24 months after teplizumab therapy. Untreated Controls are labelled as C (yellow, n=15), Responders as R (blue, n=14), and Non-Responders as NR (red, n=16).

## Supplemental Figure 5

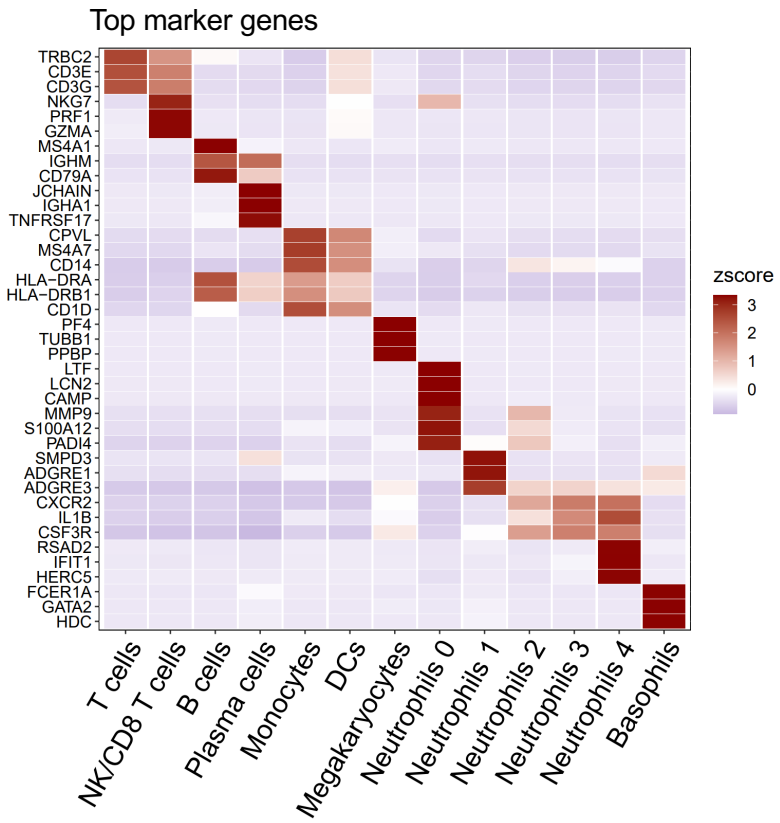


**Supplemental Figure 5. Unsupervised immune subset clustering based on RNA markers in whole blood samples from stage 3 type 1 diabetic individuals.** Heat map showing the expression of top marker genes in immune subsets of peripheral blood of stage 3 type 1 diabetic individuals.

## Supplemental Figure 6

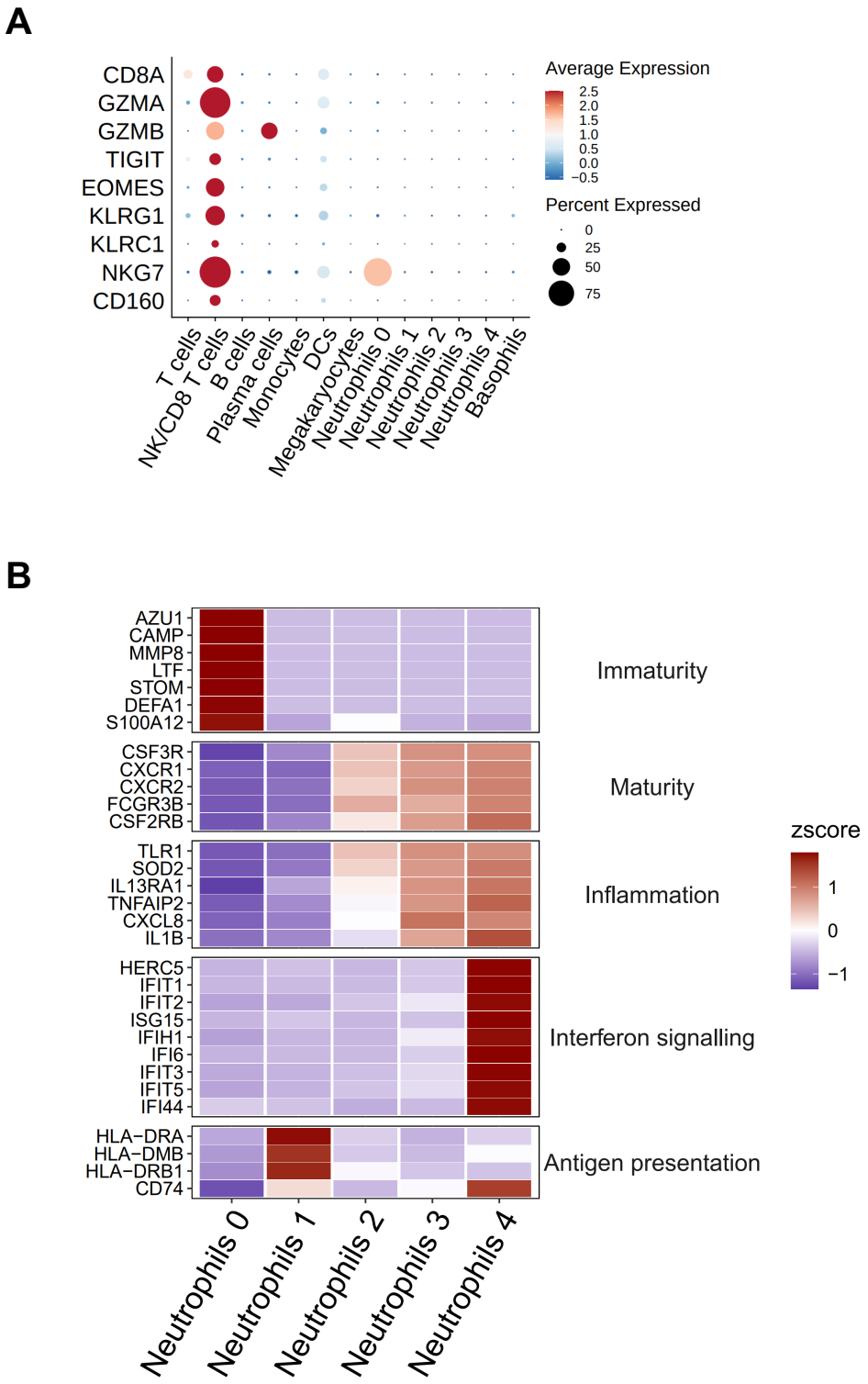


**Supplemental Figure 6. Functional gene expression in immune cells from stage 3 type 1 diabetic individuals.** (**A**) Dot plot illustrating the expression of genes associated with partial exhaustion phenotype. (**B**) Heat map displaying the expression of functional markers across different neutrophil subtypes.

# Supplemental Figure 7

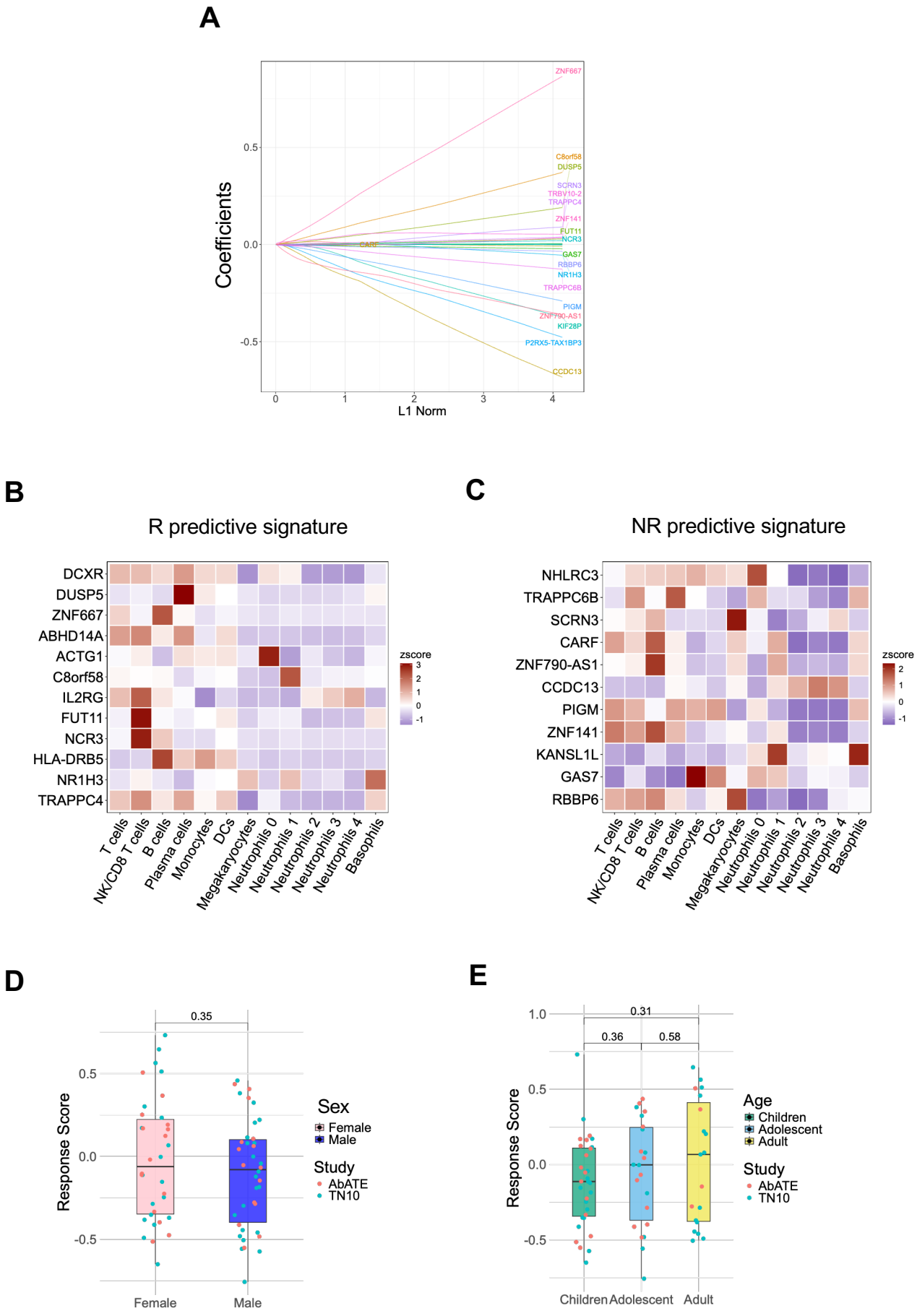

# Supplemental Figure 7

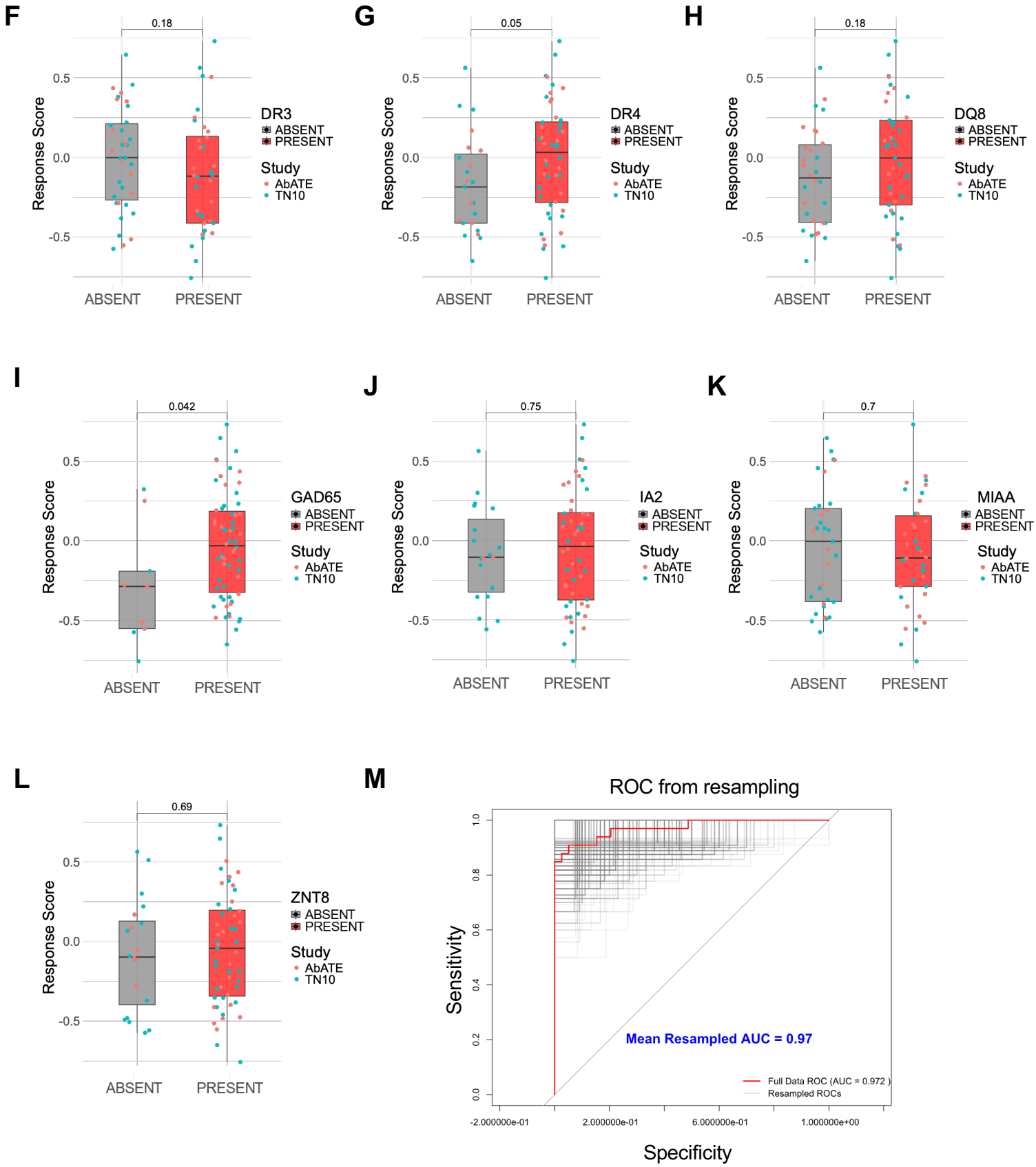

**Supplemental Figure 7. Baseline predictive response score modelling, validation and covariates.** (**A**) Coefficient paths showing changes in feature coefficients across different regularization strengths for the final selected features. (**B**) Heatmap presenting the expression levels of the individual genes with a positive coefficient comprising the "Response Score" at baseline in peripheral blood immune subsets, represented using the z-score. (**C**) Heatmap presenting the expression levels of the individual genes with a negative coefficient comprising the "Response Score" at baseline in peripheral blood immune subsets, represented using the z-score. **(D–L)** Box plots depicting baseline "Response Score" across various clinical and demographic subgroups: (**D**) Female (pink box, *n*=34) vs. male (blue box, *n*=38) participants; (**E**) Children (<12 years, green box, *n*=31), adolescents (12–18 years, blue box, *n*=22), and adults (≥18 years, yellow box, *n*=19); (**F**) Presence (red box, *n*=36) vs. absence (grey box, *n*=35) of the HLA-DR3 haplotype; (**G**) Presence (red box, *n*=48) vs. absence (grey box, *n*=23) of the HLA-DR4 haplotype; (**H**) Presence (red box, *n*=41) vs. absence (grey box, *n*=30) of the HLA-DQ8 haplotype; (**I–L**) Presence (red box) vs. absence (grey box) of autoantibodies against GAD65 (*n*=63/9), I-A2 (*n*=53/19), insulin (mIAA; *n*=38/34), and ZnT8 (*n*=51/21), respectively. Data points represent samples from the AbATE (red dots, *n*=30) and TN10 (cyan dots, *n*=42) studies. Boxes represent the median (center line) and extend from the 25$^{th}$ to 75$^{th}$ percentiles (bottom and top lines, respectively); whiskers extend from the minimum to the maximum value. The Wilcoxon Rank Sum test was used for statistical comparison. (**M**) ROC curve (AUC) overlay from 1,000 sampling of 20 random subjects from the full dataset to evaluate the predictive performance of the response score and ROC AUC of the full dataset (red curve).

**Supplementary Table 1. List of the 190 surface protein markers (antibody-derived tag or ADT) used for CITE-sequencing on CD45$^{+}$ leukocytes sorted from peripheral blood or pancreas specimen of recent-onset diabetic and anti-CD3 treated NOD mice.**

| | | | | |
|---|---|---|---|---|
| CD301b | TCRγδ | Ly49D | CD150 | CD93 |
| CD163 | IgG1-Rat-l | CD169 | CD195 | CD69 |
| TCRg2 | IgG1-Rat-k | CD39 | Ly6G | NK1-1 |
| CD304 | CD49b | CD200R3 | MERTK | CD27-A0191 |
| CD11b-mh | CD103 | IgG2b-Rat-k | CD102 | CD204 |
| CD201 | TER119 | CD49f | CD80 | CD107a |
| CD11c | CD41 | CD106 | CD34 | JAML |
| CD14 | CD21-CD35 | CD105 | IgG2a-Rat-k | FceRIα |
| CD8a | CD19 | CD3e | CD172a | TCRβ |
| Ly49H | TCRγ | IL33Ra | CD54 | CD270 |
| CD137 | Folate | CD309-A0553 | CD274 | P2X7R |
| CD138 | CD115 | IgG2b-Mouse-k | CD28 | CD279 |
| CD4 | CD62E | CD45 | CD152 | CD3 |
| Integrin | CD23 | CD71 | CD55 | TLR4 |
| TCRb5 | CD272 | CD45-A0178 | IRF4 | CD122 |
| P2RY12 | CD278 | Streptavidin-A0955 | CD223 | CD22 |
| CD117 | ENPP1 | CD62L | CD16-CD32 | IgM |
| Ly6C | CLEC4F | IgG2a-Mouse-k | CD124 | CD300LG |
| CD335 | Ly6A-Ly6E | GABRB3 | CD193 | Mac2 |
| CD192 | CD38 | KCC2 | CD197 | CD326 |
| TIGIT | CD90-A0075 | CD68 | CD185 | CD9 |
| KLRG1-mh | Siglec | CD300c-d | CD25 | IA-IE |
| Tim4 | MAdCAM1 | F4-80 | CD135 | CD314 |
| XCR1 | RORγ | CX3CR1 | 4-1BB | CD20 |
| ReceptorD4 | CD24 | ESAM | CXCR4 | CD45R-B220 |
| CD5 | CD1d | CD83 | CD196 | CD95 |
| CD8b | CD317 | CD86 | CD140a | CD127 |
| CD79b | Pan endothelial | Streptavidin-A0952 | CD370 | CD26 |
| TCRg3 | CD200R | CD226 | CD43 | CD200 |
| VSIG4 | ERK1 | CD64 | Notch | CD49d |
| CD90 | IgG2c-Rat-k | CD357 | CD309-A0554 | CD183 |
| CD36 | IgG-Hamster | CD49a | IgG2a | CD309 |
| PIRA-PIRB | H2Kb | CD44-mh | CD2 | CD309.1 |
| CD73 | CD15-mh | IgG1-Mouse-k | CD134 | Biotin |
| DR3 | CD206 | CD62P | CD29 | CD146 |
| CD371 | DLL1 | CD366 | CD11a | Streptavidin-A0953 |
| IgD | CD207-mh | CD48 | TCRβ8 | Streptavidin-A0951 |
| Ly6G-Ly6C | CD301a | CD63 | CD31 | CD278.1 |